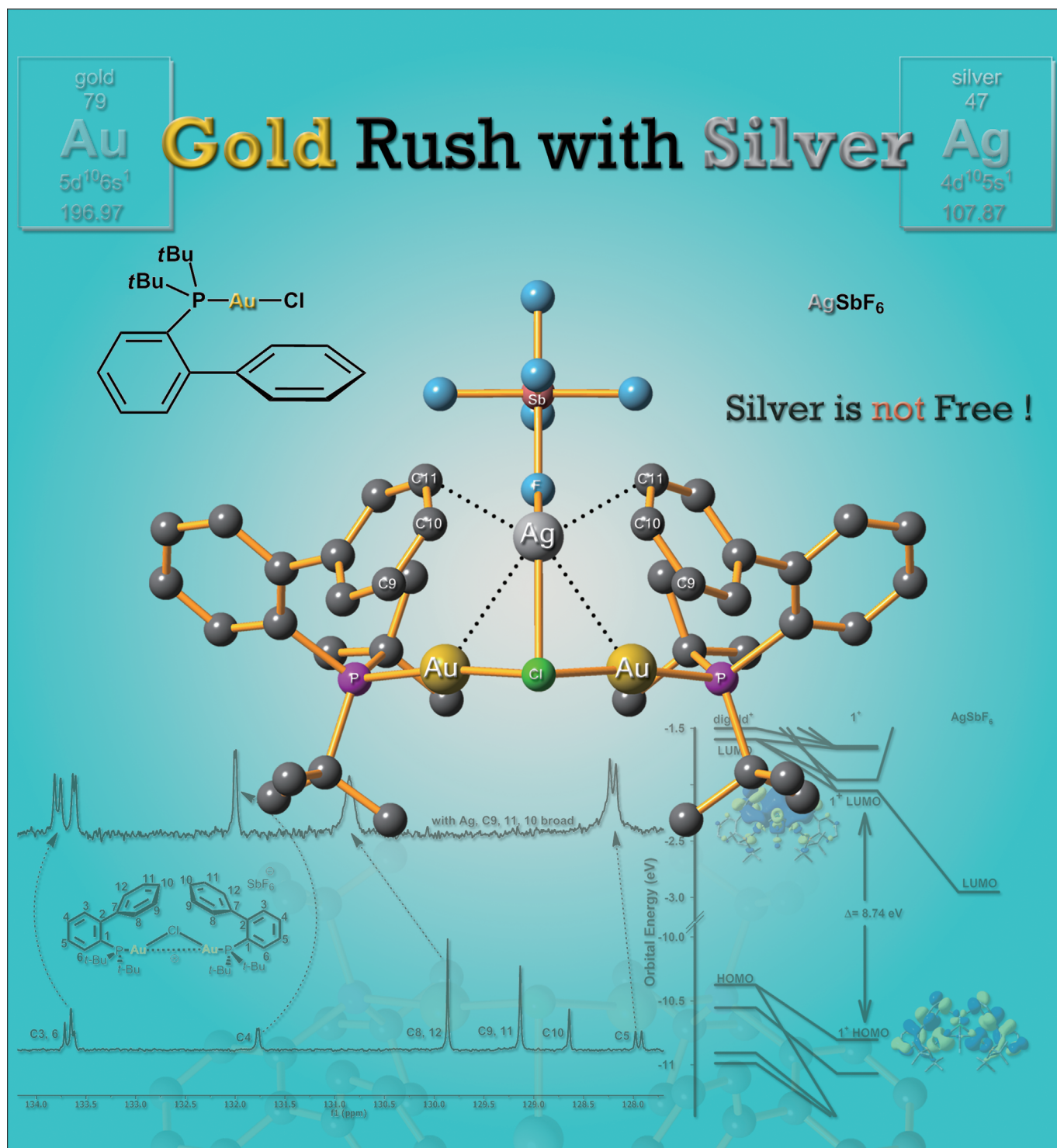


A Unique Au–Ag–Au Triangular Motif in a Trimetallic Halonium Dication: Silver Incorporation in a Gold(I) Catalyst

Yuyang Zhu, Cynthia S. Day, Lin Zhang, Katarina J. Hauser, and Amanda C. Jones*^[a]

Dedicated to Professor Hans J. Reich on the occasion of his 70th birthday



Abstract: As a result of explorations into the solution chemistry of silver/gold mixtures, a unique diphosphine trimetallic chloronium dication was discovered that incorporates silver–arene chelation and a triangular mixed gold/silver core in the solid state. Notably, it was isolated from a Celite prefiltered solution initially thought to be silver-free. The crystal structure also incorporates the coordination to silver of one fluorine atom of one SbF_6^- counterion.

The structure was compared to two new, but well-precedented, phosphine digold chloride cations. DFT calculations supported significant silver–halide and silver–arene interactions in the mixed gold/silver complex and metallophilic interactions in all three com-

Keywords: aurophilicity • cluster compounds • gold • pi interactions • silver

plexes. Comparison of computed data revealed that the ω B97X-D functional, which has a long-range corrected hybrid with atom–atom dispersion corrections, gave a better fit to the experimental data compared with the PBE0 functional, which has previously failed to capture aurophilic interactions. Preliminary studies support the presence of the mixed gold/silver structure in solution.

Introduction

Silver salts are routinely used in combination with gold chloride complexes for use as catalysts^[1] and in the preparation of organogold π complexes.^[2] Although experimental procedures have been reported that include a filtration step to remove the AgCl precipitate, many presume silver does not remain in solution and can thus be eliminated from discussions of catalytic cycles, a conclusion also supported by control experiments that demonstrate the lack of catalytic activity of silver alone. A growing body of recent work, however, is demonstrating the distinct influence of silver on gold-catalyzed reactions, such as the observation of mixed Au–Ag intermediates in reaction solutions^[3] and the impact of silver on rates^[3] and selectivities.^[4] Additionally, there is a growing trend toward the development of silver-free catalysts, due to the ambiguity of silver involvement and stoichiometry.^[5,6] In our efforts to prepare mechanistically relevant gold complexes^[7] from the preparative combination of phosphine gold chlorides and silver salts, we have encountered situations where the expectation of “quantitative precipitation of AgCl”^[10a] was inconsistent with our observations. We thus sought to more carefully explore the solution chemistry of silver/gold mixtures. From our effort to further probe the phenomena, we report on three new gold chloride structures: a unique trimetallic chloronium dication (coordination mode as in **B**, Figure 1) and two monomeric digold chloronium ions (coordination mode as in **C**₁, Figure 1).

The first example of a mixed $\text{Au}^{\text{I}}\text{–Ag}^{\text{I}}$ chloronium cation was reported in the solid state by Yip and co-workers.^[8] In their studies, a 2:1 ratio of phosphine gold(I) chloride/AgSbF₆ and recrystallization by slow diffusion between CH₂Cl₂ and THF solutions yielded crystalline cationic coor-

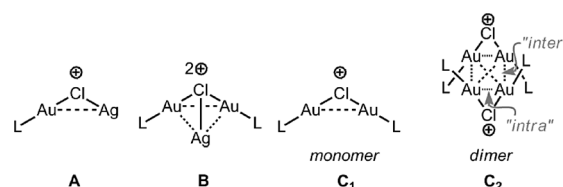


Figure 1. Bonding in cationic monomeric and polymeric phosphine gold chloride complexes.

dination polymers with a 4:1 gold/silver stoichiometry (coordination mode as in **A**, Figure 1), demonstrating that, under appropriate conditions, combination of a gold(I) halide and silver salt would not result in quantitative halide abstraction and selective precipitation of silver chloride. This contrasted to the work of Uson^[9] and Schmidbauer,^[10] who observed formation of Au_2X^+ halonium ion monomers and dimers from mixtures deficient in silver salt (coordination mode as in **C**₁ and **C**₂, Figure 1). Recently, a silver(I)-coordinated gold(I) chloride was isolated from a Celite-filtered 1,2-dichloroethane solution of $[(\text{L})\text{AuCl}]/\text{AgSbF}_6$ ($\text{L} = 1,3\text{-bis}[2,6\text{-bis}[\text{bis}(4\text{-tert-butylphenyl)methyl}]\text{-4-methylphenyl}]\text{-2,3-dihydro-1H-imidazol-2-ylidene}$), a procedure also generally believed to result in efficient removal of silver chloride (coordination mode as in **A**, Figure 1).^[11] Those authors propose an equilibrium process to explain the retention of small amounts of AgCl in solution. Silver has also been shown to coordinate to $(\text{LAu})_3\text{S}$ cations at sulfur (Au_3AgS square pyramid).^[12]

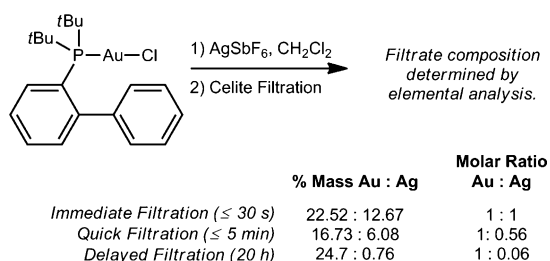
Results and Discussion

In our recent efforts to synthesize gold(I) enol ether complexes,^[7] we adopted a procedure of mixing phosphine gold(I) chlorides with AgSbF₆ in CH₂Cl₂ followed by filtration through Celite. According to experimental procedures described in the literature, this was expected to coincide with an initial quantitative precipitation of solid AgCl and formation of $\text{R}_3\text{PAu}^+\text{SbF}_6^-$, which would remain in solution.^[13] Additionally, we noted (albeit in hindsight) that such complexes, deficient in coordinating ligands, should also be highly unstable. For example, many triarylphosphine gold

[a] Y. Zhu, Dr. C. S. Day, L. Zhang, K. J. Hauser, Prof. A. C. Jones
Chemistry Department, Wake Forest University
Salem Hall, Box 7486 (USA)
Fax: (+1) 336-758-4656
E-mail: jonesac@wfu.edu

Supporting information for this article is available on the WWW under <http://dx.doi.org/10.1002/chem.201302152>.

cations are clearly unstable,^[14] though ligand structure and choice of counteranion surely impact this. We were thus surprised to observe formation of a second precipitate upon addition of the strongly coordinating enol ether, without any major negative impact on the synthesis of the desired complexes. Upon closer examination of our procedure, we visually confirmed formation of a precipitate upon mixing the gold and silver salts; however, the solid collected after filtration and solvent evaporation amounted to 96% recovery of the total initial mass. An 83.6% theoretical yield (w/w) is expected after quantitative removal of AgCl precipitate. Elemental analysis of the solid collected showed a 1:1 stoichiometry of gold/silver, revealing an intimate association of gold and silver was retained in solution (Immediate Filtration, Scheme 1). Thus, visible assessment of precipitates can be misleading. See the Supporting Information for pictures of solutions before and after filtration.



Scheme 1. Elemental analyses of Celite-filtered mixtures (0.05 mmol gold/silver in 0.6–1 mL CH_2Cl_2).

We considered the possibility that precipitation of AgCl might be a slow process and indeed found it to be sensitive to time. Little to no AgCl precipitates when the filtration is done immediately (within 30 s). Approximately half of the AgCl precipitates when the filtration is done quickly (within 5 min; Quick Filtration, Scheme 1). Stirring for 20 h removed most of the silver, but a trace remained (Delayed Filtration, Scheme 1). In contrast, Shi and co-workers used X-ray photoelectron spectroscopy (XPS) to analyze Celite-filtered mixtures of $[(\text{Ph}_3\text{P})\text{AuCl}]/\text{AgSbF}_6$ and $[(\text{IPr})\text{AuCl}]/\text{AgSbF}_6$ (IPr = 1,3-Bis(2,6-diisopropylphenyl)imidazol-2-ylidene) and showed Celite to be completely effective at removing silver, even when the initial mixtures contained an excess of silver salt.^[4] We found that similar quick filtration experiments with diethyl ether, acetone, and THF yielded filtrates that all retained 1–3% silver by elemental analysis.

When solutions of $[(t\text{Bu})_2(o\text{-biphenyl})\text{P}]\text{AuCl}/\text{AgSbF}_6$ were placed in a -10°C freezer, crystals of a new mixed silver–gold chloride complex ($\mathbf{1}\cdot\text{CH}_2\text{Cl}_2$) readily formed (coordination mode **B**, Figure 1; ORTEP plot, Figure 2). Complex $\mathbf{1}\cdot\text{CH}_2\text{Cl}_2$ can be characterized as a silver-coordinated digold chloronium ion. It is more closely related to the digold halonium ions reported by Schmidbaur and co-workers (coordination mode as in **C**₁ and **C**₂, Figure 1)^[10] than to the mixed complex reported by Yip, wherein silver cations link individual phosphine gold chloride units in a polymeric

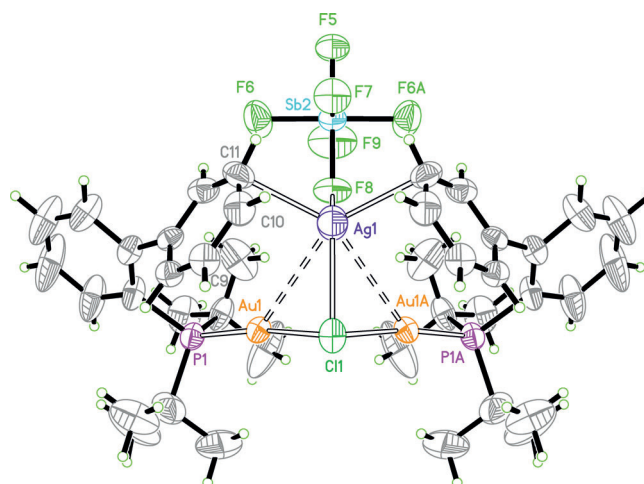
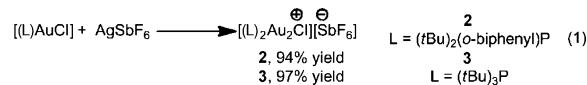


Figure 2. ORTEP plot of $\mathbf{1}\cdot\text{CH}_2\text{Cl}_2$. Disordered solvent molecule (CH_2Cl_2) and counterion (SbF_6^-) omitted. Ellipsoids are shown at 50% probability level.

array (coordination mode **A**, Figure 1).^[8] Striking features of $\mathbf{1}\cdot\text{CH}_2\text{Cl}_2$ include the coordination of one equivalent of the “noncoordinating” counteranion SbF_6^- and the chelation of two biphenyl groups to silver (further discussion below).

For comparison to the related digold chloronium salts, we prepared complexes **2** and **3** [Eq. (1)].^[15] Compounds **2** and



3 were also recrystallized by slow diffusion of hexanes into CH_2Cl_2 at -10°C to yield solvated complexes $\mathbf{2}\cdot\frac{1}{2}\text{H}_2\text{O}$ and $\mathbf{3}\cdot\text{CH}_2\text{Cl}_2$ (ORTEP plots in Figure 3 and Figure 4).^[16]

In the solid state, $\mathbf{2}\cdot\frac{1}{2}\text{H}_2\text{O}$ and $\mathbf{3}\cdot\text{CH}_2\text{Cl}_2$ are monomeric and share many similarities with the series of triarylphosphine halide complexes previously reported by Schmidbaur.^[10] For some of those structures, dimeric salts are ob-

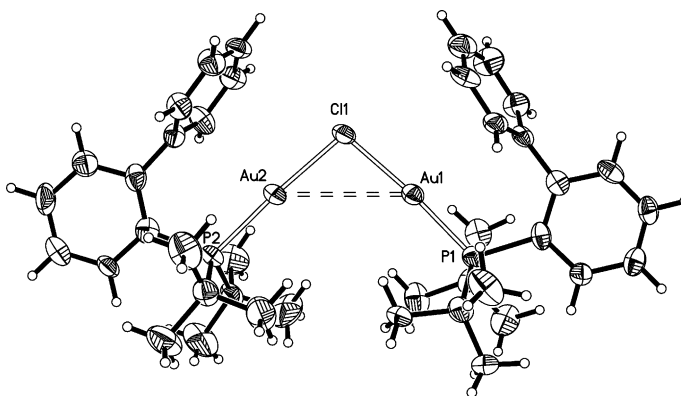


Figure 3. ORTEP plots of $\mathbf{2}\cdot\frac{1}{2}\text{H}_2\text{O}$. Water molecule and counterion (SbF_6^-) omitted. Ellipsoids are shown at 50% probability level.

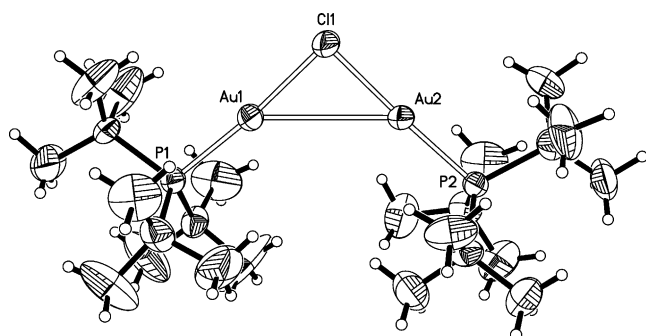


Figure 4. ORTEP plots of **3**·CH₂Cl₂. Solvent molecule and counterion (SbF₆[−]) omitted. Ellipsoids are shown at 50% probability level.

served in the solid state (dimer **C**₂, Figure 1). Dimerization is proposed to be driven by aurophilic interactions that counter balance Coulomb repulsion and is predicted to be highly sensitive to the size of the counteranion. Specifically, complexes with the smaller counterions BF₄[−] and ClO₄[−] are monomeric, while those with the SbF₆[−] counterion are dimeric.^[10a,b] The current structures demonstrate that ligand size and/or donor strength can also make dimer formation unfavorable.

The Au–Au distances that are considered to reveal “aurophilic interactions” have been defined by Schmidbauer to be within the range of 2.5–3.5 Å.^[17] In complexes where multiple gold atoms coordinate around a single central atom, aurophilic interactions are also indicated by acute Au–X–Au angles (< 90°). According to these structural features, digold **3**·CH₂Cl₂ (Au–Au = 3.2983(6) Å, Au–Cl–Au = 89.55(7)°) displays a more significant aurophilic interaction than digold **2**·¹/₂H₂O (Au–Au = 3.543 Å, Au–Cl–Au = 97.73(9)°; Table 1). The Au–*ipso* distance (3.028 Å) in **2**·¹/₂H₂O is shorter than that observed in the neutral L–Au–Cl parent (3.16 Å) and similar to the corresponding cationic acetonitrile complex (3.04 Å), suggesting arene interactions are increased by the positive charge of the complex.^[18]

As noted by Gagné,^[3] coordination of Ag⁺ is not anticipated to perturb the parent structure, and the similar structural parameters of the Au–Cl–Au core of **1**·CH₂Cl₂ and **2**·¹/₂H₂O confirm this (Au–Cl lengths within 3 esd, Au–Cl–

Table 1. Select bond lengths [Å] and angles [°] for **1**·CH₂Cl₂, **2**·¹/₂H₂O, and **3**·CH₂Cl₂.

	1 ·CH ₂ Cl ₂	2 · ¹ / ₂ H ₂ O	3 ·CH ₂ Cl ₂
Au–Cl–Au	98.47(7)	97.73(9)	89.55(7)
Au–Au ^[a]	3.554	3.543	3.2983(6)
Au1–Cl1	2.3461(12)	2.350(3)	2.344(2)
Au2–Cl1	–	2.353(3)	2.339(2)
Au–Ag ^[a]	3.3202(8)	–	–
Ag–F ^[a]	2.486(5)	–	–
Ag–Cl	2.637(2)	–	–
Ag–C11 ^[a]	2.497(6)	–	–
Ag–C10	2.718(5)	–	–

[a] Sum of VDW radii: Au(1.66) and Cl(1.75) is 3.41 Å, Au and Ag(1.72) is 3.38 Å, Ag and Cl is 3.47, Ag and F(1.47) is 3.19, Ag and C(1.70) is 3.42 Å.^[19]

Au angles within 5 esd; esd = estimated standard deviation). However, the presence of the coordinating silver does significantly perturb the orientation of both *t*Bu₂(*o*-biphenyl) ligands, twisting them out of the Au–Cl–Au plane in order to chelate with the silver atom. Arene coordination in silver complexes is a well-precedented phenomenon,^[20] indeed the complex isolated by Straub et al. (coordination mode **A**, Figure 1) contained an N-heterocyclic carbene ligand with arene substituents that chelated to silver,^[11] and a recent mixed gold(III)–silver complex also shows arene–silver interactions.^[21] According to Kochi’s hapticity equation^[22] the silver coordinates in a η^{1,2} manner with silver’s closest contact being the *meta* carbon of the second biphenyl arene (C11–Ag1 = 2.497(6) Å). Kochi has analyzed crystallographic data for a number of silver(I) complexes with aromatic donors and found that all of them fell within a narrow range of structural parameters (Table 2). Parameters measured for **1**·CH₂Cl₂ show a good fit; the Ag–arene distance is within the expected range; the other values are just outside it. This suggests we are observing “true” arene–silver coordination rather than an interaction that is coincidentally constrained by the geometry of the complex.

Table 2. Comparison of structural features in **1**·CH₂Cl₂ to known complexes using Kochi’s parameters to measure optimal depth penetration for silver(I)–arene coordination.^[a]

	1 ·CH ₂ Cl ₂	Known complexes
d [Å]	2.41 ± 0.05 (2.411)	β [°C] = 32 ± 3 (37.4)
Δ [Å]	1.53 ± 0.2 (1.845)	α [°C] = 95 ± 3 (91.5)

[a] Numbers outside brackets are the range reported in ref. [20]; numbers in brackets are those measured in **1**·CH₂Cl₂. d = distance of silver from the mean plane of the aromatic ring; Δ = deviation from the centroid axis; α = “grab” angle between the planes of the coordinated aromatic ring.

An additional notable feature of **1**·CH₂Cl₂ is the coordination of one fluorine atom of the SbF₆[−] anion to silver. The Ag1–F8 distance (2.486(5) Å) in **1**·CH₂Cl₂ is nearly identical to that observed in crystalline AgSbF₆, in which each unit cell contains a silver atom equivalently coordinated to six F atoms from six different SbF₆[−] units in a distorted octahedron (Ag–F = 2.505(2) pm).^[23]

In order to determine whether the silver–arene interaction is retained in solution, we first analyzed the NMR spectra of solutions of **1** and **2**. The ¹³C shifts of both complexes were assigned by comparison to the parent [((*t*Bu)₂(*o*-biphenyl)P)AuCl].^[24] Figure 5 shows an inset of the relevant shift region for **1** and **2**; the aromatic ring that shows coordination to silver presents significant differences. The *meta* and *para* carbon atoms (C9/C11, C10), which show contacts in the crystal structure, are absent altogether, while the *ortho* carbon atoms (C8/C12) are broadened and downfield. The other carbon atoms (C1–C7) showed minor changes. Although the specific cause of this dynamic effect is not

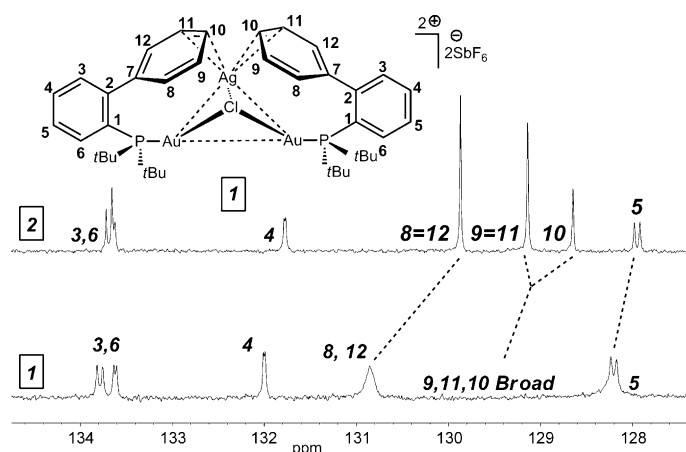


Figure 5. Inset of ^{13}C NMR spectra of **1** (12.6 mm) and **2** (35.7 mm) in CD_2Cl_2 at 25°C (carbon labels based on X-ray data of **1**· CH_2Cl_2).

known, it is strongly indicative of an interaction that is maintained in solution. For additional evidence, we performed silver titration experiments and measured the changes in UV/Vis absorption. Key differences between the spectra of **1** and **2**, as well as the increasing similarity between the spectra of **1** and **2** with increasing AgSbF_6 , support an interaction in solution. However, solubility problems at high silver concentrations prevented a more careful determination of the binding constant.^[25]

In addition to the implications this complex has for the preparation of “silver-free” solutions, we were also intrigued by the unique bonding features in **1**. The isolobality of cationic gold and protons has led to extremely fruitful explorations in reactive intermediate chemistry;^[26] many gold analogues of classic high-energy species have been prepared, including a trigold monocation (isolobal to H_3^+),^[27] gold analogues of hypervalent carbon,^[28] and gold oxoniums (analogues of H_3O^+ and H_4O^{2+}).^[29,17a] Indeed, the digold choronium complexes **2** and **3** are analogues of H_2Cl^+ .^[30] Gas-phase studies on H_3Cl^{2+} show that dissociation to H_2Cl^+ and H^+ is exothermic; these higher coordinated halonium dications have been implicated by exchange studies, but not directly observed. Thus, complex **1** represents a rare case of a simple tricoordinate halonium dication, and the first example of one incorporating gold and silver around the chlorine atom. The asymmetric pyramidal shape contrasts the trigonal planar coordination about chlorine in N-heterocyclic carbene ligated $[\text{Ag}_3\text{Cl}]^{2+}$ and $[\text{Ag}_3\text{I}]^{2+}$ complexes,^[31] and the T-shape coordination seen in a neutral mixed gold(III)–silver(I) phosphide complex (Ag_3Cl core).^[32]

To gain further insight into the nature of the interactions in these complexes, DFT calculations were applied to mono-cations of **1–3** (one SbF_6^- not included, denoted $\mathbf{1}^+–\mathbf{3}^+$).^[25] Use of the PBE0 functional^[33,34] did not produce optimized structures that fit very well with the X-ray data. In particular, significant disagreement was observed for the metal–metal bond lengths and Au–Cl–Au bond angles (Table 3). This is consistent with the observation that DFT sometimes

Table 3. Select computed data and bond orders in $\mathbf{1}^+$, $\mathbf{2}^+$, and $\mathbf{3}^+$.

	$\omega\text{B97X-D}$ (Δ) ^[a]	PBE0 (Δ) ^[a]	Mayer bond order	Wiberg bond index
$\mathbf{1}^+$, Au–Ag	3.559 (0.24)	3.698 (0.38)	0.05	0.062
$\mathbf{1}^+$, Au–Au	3.687 (0.13)	3.902 (0.35)	−0.0077	0.108
$\mathbf{1}^+$, Au–Cl–Au	99.0 (0.5)	106.7 (8.2)		
$\mathbf{2}^+$, Au–Au	3.599 (0.06)	3.750 (0.21)	0.05	0.123
$\mathbf{2}^+$, Au–Cl–Au	97.1 (0.6)	102.1 (4.4)		
$\mathbf{3}^+$, Au–Au	3.355 (0.06)	3.642 (0.34)	0.06	0.130
$\mathbf{3}^+$, Au–Cl–Au	88.5 (1)	98.2 (8.6)		

[a] $\Delta = |\text{calculated length} [\text{\AA}] - \text{crystal length} [\text{\AA}]|$, or $|\text{calculated angle} [^\circ] - \text{crystal angle} [^\circ]|$.

fails to capture aurophilic interactions.^[34] Improvements could be made by use of the $\omega\text{B97X-D}$ functional, which has a long-range corrected hybrid with atom–atom dispersion corrections.^[35,36] The computationally optimized structures of $\mathbf{1}^+–\mathbf{3}^+$ are in excellent agreement with the X-ray data for $\mathbf{2} \cdot \frac{1}{2}\text{H}_2\text{O}$ and $\mathbf{3} \cdot \text{CH}_2\text{Cl}_2$ and in good agreement for **1**· CH_2Cl_2 . Although the fit is good, all computed values are too high (they still slightly underestimate metallic interactions).

Computational analysis of dimers $[\{(\text{PPh}_3)_2\text{Au}_2\text{X}\}_2]^{2+}$ ($\text{X} = \text{F}, \text{Br}, \text{Cl}, \text{I}$)^[37] and structural features for $[\{(\text{PPh}_3)_2\text{Au}_2\text{Cl}\}_2][\text{SbF}_6]_2$ ^[10a,b] have suggested weak to no aurophilic interactions between the two gold atoms within a monomeric unit (see **C**₂, “intra”, Figure 1) and significant aurophilic interactions in the dimers between the gold atoms of the monomer unit (see **C**₂, “inter”, Figure 1). This is reflected in the Mayer bond order (MBO);^[38] it is approximately 0.229–0.241 between the gold atoms of each monomer unit (“inter”) and approximately 0.011–0.039 between the gold atoms within the monomer unit (“intra”).^[39] It is structurally reflected in the short “inter” bond distance ($\approx 3.08 \text{ \AA}$) and longer “intra” bond distance ($\approx 3.66 \text{ \AA}$) observed for $[\{(\text{PPh}_3)_2\text{Au}_2\text{Cl}\}_2][\text{SbF}_6]_2$ in the solid state. On the basis of solid-state structural features, **3**· CH_2Cl_2 presents a stronger aurophilic interaction compared with $\mathbf{2} \cdot \frac{1}{2}\text{H}_2\text{O}$ (see above), yet the Au–Au MBOs of the corresponding cations were small and nearly identical (0.05 for $\mathbf{2}^+$ and 0.06 for $\mathbf{3}^+$). For $\mathbf{1}^+$, the MBO results were puzzling (further discussion below); the Au–Au MBO was small and negative, (−0.0077), while the Au–Ag MBO was small (0.05).

According to a charge decomposition analysis (CDA) of $\mathbf{1}^+$ (Figure 6), the highest-occupied Kohn–Sham orbital (HOMO) is dominated by the digold fragment (95%).^[40] Percentages are of the total electron density and are calculated from Mulliken population analysis.^[41] The LUMO is composed of both the digold (45%) and Ag (55%) fragment. This result suggests both digold and silver fragments participate in the excited state of the Au–Ag–Au structure.^[27,34,42] The HOMO–LUMO gap is calculated at 8.74 eV, larger than that of the trigold monocation.^[27]

To gain an understanding of the localized description of the electronic structure of $\mathbf{1}^+$, natural bond orbital (NBO) analysis was performed.^[43] A relatively large noncovalent interaction was found between the Cl lone pairs and the virtu-

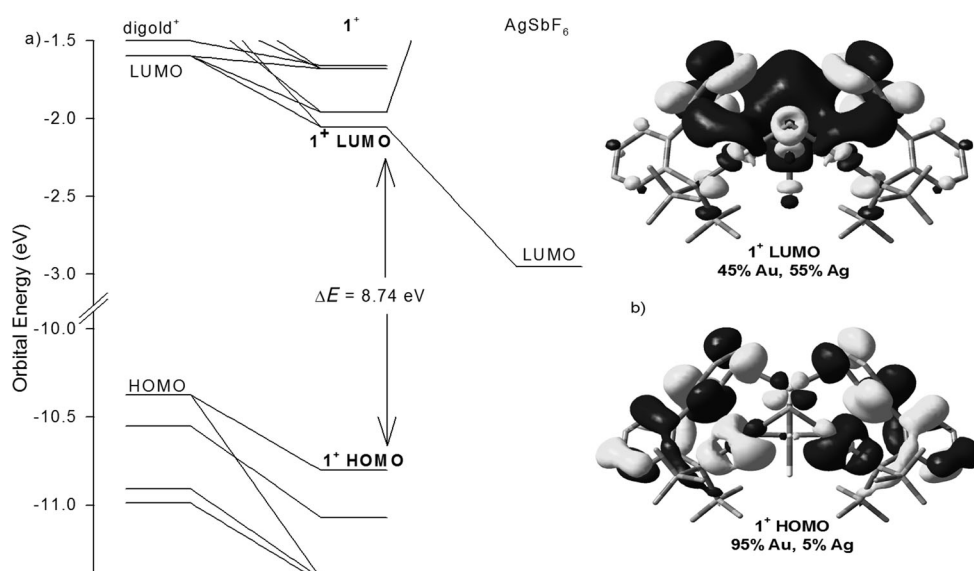


Figure 6. a) Partial CDA of Kohn–Sham orbital energy diagram of **1**⁺; b) selected orbitals (0.02 a.u.) and percentage compositions based on Mulliken population analysis.

al orbitals of Ag (the largest second-order energy lowering $\Delta E^{(2)}$ is 18.9 kcal mol⁻¹, Table 4) compared with the noncovalent interactions between aromatic C10–C11 $\sigma(\text{BD}_1)$ or $\pi(\text{BD}_2)$ orbitals and virtual orbitals of Ag (largest $\Delta E^{(2)}$ of σ orbitals and virtual orbitals of Ag is 4.2 kcal mol⁻¹; largest $\Delta E^{(2)}$ of π orbitals and virtual orbitals of Ag is 5.6 kcal mol⁻¹). These are also indicative of a significant interaction between silver, chloride, and the chelating aromatic rings.

The MBOs of **1**⁺ (in particular the negative value for Au–Au) challenge our ability to make conclusions about the relative strength of Au–Au and Au–Ag bonds in these complexes. Compared to Mulliken charges (upon which Mayer bond orders are based), natural population analysis (NPA) has been shown to better describe electron distribution in compounds of high ionic character.^[43b] Thus, we also calculated Wiberg bond orders in the NPA (Table 3).^[44] Although auro-argentophilic interactions are reported to be stronger than aurophilic interactions,^[3] the Wiberg bond indices do

not show this trend. Instead, the Ag–Au bond order is smallest, and the Au–Au bond order increases from **1**⁺ to **3**⁺. From either perspective, the metallophilic interactions are moderate.

Conclusion

In summary, we have identified a new structural motif incorporating silver and gold coordinated to a central chloride anion. Although there is much evidence that silver additives can affect the course of gold-catalyzed reactions, very little is known about the structures involved. The popularity of the Buchwald-type biphenylphosphines and the special chelating properties revealed herein suggest that silver involvement may be of particular significance to reactions utilizing such ligands. Additionally, a sure prerequisite to determining the role of mixed complexes in catalysis is the ability to

synthesize and characterize them. Biphenylphosphine may provide an organizational force to facilitate the isolation of additional mechanistically relevant mixed complexes.

The formation of **1–3** from Au/Ag mixtures is likely driven less by stability from metallophilic interaction and more by the instability of uncoordinated $[(\text{L})\text{Au}]^+$. The first $\frac{1}{2}$ equivalent of chloride is presumably abstracted quite smoothly from

Table 4. Selected NBOs (0.02 a.u.) of **1**⁺ computed at optimized gas-phase structure using ω B97X-D functional. Interaction of a) occupied lone pair (LP_2 , $\text{sp}^{7.55}$) on Cl with unoccupied orbital (LP_7^*) on Ag; b) two aromatic C10–C11 σ orbitals (BD_1) with LP_9^* on Ag; c) two aromatic C10–C11 π orbitals (BD_2) with LP_8^* on Ag.

a)	b)	c)
Cl (LP_2) → Ag (LP_7^*) 18.92 kcal mol ⁻¹	2 C10–C11 (σ) → Ag (LP_9^*) 2 × 4.2 kcal mol ⁻¹	2 C10–C11 (π) → Ag (LP_8^*) 2 × 5.6 kcal mol ⁻¹

[a] Occupied orbitals are represented by solid spheres; unoccupied orbitals by mesh spheres. NBO overlap graphs were made by VMD 1.9.1.

[(L)AuCl] to form **2** and **3** (consistently in high yield); the initially formed [(L)Au]⁺ is stabilized by coordination to remaining [(L)AuCl]. Complexes like **2** and **3** are certainly catalytically active, as was shown for related complexes by Hashmi and co-workers.^[45] Addition of cyclohexadiene, methoxypropene, and acetonitrile to solutions of **2** also support the conclusion that they represent a labile source of cationic gold (each substrate displaced [(L)AuCl] to varying extents).^[25] The observation that enol ethers drive additional displacement of AgCl from **1** suggests that, in the presence of substrate, silver incorporation is likely minimal. Nevertheless, complex **1** represents both a snapshot of the early stages of halide abstraction^[11] and potentially a mechanism by which silver can be reincorporated into catalyst structures. Work is ongoing in our laboratory to determine the role of these structures in catalysis.

Experimental Section

[(*t*Bu)₂(*o*-biphenyl)P]₂Au₂ClAg(SbF₆)][(SbF₆)-CH₂Cl₂ (1-CH₂Cl₂)**: In a glove box, a slurry of **[(*t*Bu)₂(*o*-biphenyl)P]AuCl** (54 mg, 0.05 mmol) and AgSbF₆ (35.4 mg, 0.05 mmol) was filtered through Celite in CH₂Cl₂ (0.6 mL) after stirring briefly (30 s). The solution was sealed and placed in a -10 °C freezer. Crystals began to form after 8 h and increased after 24 h. The white crystals were filtered and dried in vacuo (12.3 mg, 14.4%). ¹H NMR (500 MHz, CD₂Cl₂, 25 °C): δ = 7.89 (td, *J* = 7.9, 1.8 Hz, 2H), 7.61 (m, 6H), 7.51 (t, *J* = 7.0 Hz, 4H), 7.32–7.29 (m, 2H), 7.26 (d, *J* = 7.1 Hz, 4H), 1.40 ppm (d, *J* = 16.3, 36 Hz); ¹³C NMR (125 MHz, CD₂Cl₂, 25 °C): δ = 148.9 (br), 143.9 (br), 133.8 (d, *J* = 7.7 Hz), 133.6 (d, *J* = 3.8 Hz), 132.0 (d, *J* = 2.5 Hz), 130.9 (s), 128.2 (d, *J* = 7.9 Hz), 124.3 (d, *J* = 50.4 Hz), 38.8 (d, *J* = 26.1 Hz), 31.1 ppm (d, *J* = 6.2 Hz); ³¹P{¹H} NMR (202.45 MHz, CD₂Cl₂, 25 °C): δ = 62.8 ppm; elemental analysis calcd (%) for C₄₁H₅₆AgAu₂Cl₃F₁₂P₂Sb₂ (1690.49): H 3.34, C 29.13, Au 23.30, Ag 6.38; found: H 3.29, C 29.09, Au 23.18, Ag 6.30.**

[(*t*Bu)₂(*o*-biphenyl)P]₂Au₂Cl[SbF₆] **(2): In a glove box, methylene chloride (0.6 mL) was added to a vial containing AgSbF₆ (8.7 mg, 0.025 mmol) and (*t*Bu)₂(*o*-biphenyl)phosphine gold chloride (27 mg, 0.05 mmol). The solution was stirred for 1 h then filtered through Celite. The filtrate was concentrated under reduced pressure to yield a white solid (29.6 mg, 93.5%). ¹H NMR (500 MHz, CD₂Cl₂, 25 °C): δ = 7.93–7.85 (m, 2H), 7.64–7.55 (m, 4H), 7.55–7.50 (m, 2H), 7.42–7.36 (m, 4H), 7.34–7.29 (m, 2H), 7.19–7.08 (m, 4H), 1.40 ppm (d, *J* = 16.2, 36 Hz); ¹³C NMR (125 MHz, CD₂Cl₂, 25 °C): δ = 149.5 (d, *J* = 12.3 Hz), 143.0 (d, *J* = 6.7 Hz), 133.7 (d, *J* = 12.3 Hz), 133.6 (d, *J* = 4.1 Hz), 131.8 (d, *J* = 2.4 Hz), 129.9 (s), 129.1 (s), 128.6 (s), 128.0 (d, *J* = 7.7 Hz), 124.7 (d, *J* = 49.2 Hz), 38.5 (d, *J* = 26.1 Hz), 31.1 ppm (d, *J* = 6.4 Hz); ³¹P{¹H} NMR (202.45 MHz, CD₂Cl₂, 25 °C): δ = 62.1 ppm; elemental analysis calcd (%) for C₄₀H₅₄Au₂ClF₆P₂Sb (1261.94): H 4.31, C 38.07; found: H 4.24, C 38.09.**

[(*t*Bu)₃P]₂Au₂Cl[SbF₆] **(3): In a glove box, methylene chloride (0.6 mL) was added to a vial containing AgSbF₆ (9.1 mg, 0.026 mmol) and (*t*Bu)₃phosphine gold chloride (22.4 mg, 0.05 mmol). The solution was stirred for 1 hour then filtered through Celite. The filtrate was concentrated under reduced pressure to yield a white solid (26.4 mg, 96.7%). ¹H NMR (500 MHz, CD₂Cl₂, 25 °C): δ = 1.55 ppm (d, *J* = 14.6 Hz, 54H); ¹³C NMR (125 MHz, CD₂Cl₂, 25 °C): δ = 40.61 (d, *J* = 20.7 Hz), 32.51 ppm (d, *J* = 3.9 Hz); ³¹P{¹H} NMR (202.45 MHz, CD₂Cl₂, 25 °C): δ = 95.2 ppm; elemental analysis calcd (%) for C₂₄H₅₄Au₂ClF₆P₂Sb (1069.77): H 5.09, C 26.95, found: H 4.99, C 27.02.**

Calculations: Density functional theory calculations were performed within the program Gaussian 09 (see Supporting Information for full references). Model compounds were chosen directly from the X-ray data and differed only by the omission of solvent molecules and one SbF₆⁻ counterion. The 6–31G** basis set was applied to nonmetal atoms.^[46] The

Stuttgart 97 effective core potential and basis set was employed for Au, Ag, and Sb metal atoms, in which scalar relativistic effects are treated implicitly.^[47] Vibrational frequency calculations found all vibrational frequencies to be real. The geometries were optimized in the gas phase without symmetry constraint using the ωB97X-D functional,^[51] which has the long-range corrected hybrid with atom–atom dispersion corrections. NBO calculations were done using NBO Version 3.1 which is included in Gaussian 09.

Acknowledgements

Acknowledgements are made to Wake Forest University for start-up funds, Dr. Brian Esselman (UW) for helpful discussions, Tian Lu (USTB) for helpful suggestions on using Multiwfn 2.6.1, Dr. Marcus W. Wright (WFU) for assistance in the NMR facility, Prof. Akbar Salam (WFU) and Dr. David Chin (WFU) for support in the use of Gaussian 09, and the National Science Foundation for the funding of the purchase of X-ray equipment (Award No. 0234489). Computations were performed on the WFU DEAC Cluster, a centrally managed resource with support provided in part by the University.

- [1] For some reviews, see: a) A. Fürstner, P. W. Davies, *Angew. Chem.* **2007**, *119*, 3478–3519; *Angew. Chem. Int. Ed.* **2007**, *46*, 3410–3449; b) A. Arcadi, *Chem. Rev.* **2008**, *108*, 3266–3325; c) E. Jiménez-Núñez, A. M. Echavarren, *Chem. Rev.* **2008**, *108*, 3326–3350; d) D. J. Gorin, B. D. Sherry, F. Dean Toste, *Chem. Rev.* **2008**, *108*, 3351–3378.
- [2] H. Schmidbaur, A. Schier, *Organometallics* **2010**, *29*, 2–23.
- [3] D. Weber, M. R. Gagné, *Org. Lett.* **2009**, *11*, 4962–4965.
- [4] D. Wang, R. Cai, S. Sharma, J. Jirak, S. K. Thummanapelli, N. G. Akhmedov, H. Zhang, X. Liu, J. L. Petersen, X. Shi, *J. Am. Chem. Soc.* **2012**, *134*, 9012–9019.
- [5] H. Schmidbaur, A. Schier, *Z. Naturforsch. B.* **2011**, *66b*, 329–350.
- [6] S. Gaillard, J. Bosson, R. S. Ramón, P. Nun, A. M. Z. Slawin, S. P. Nolan, *Chem. Eur. J.* **2010**, *16*, 13729–13740.
- [7] Y. Zhu, C. S. Day, A. C. Jones, *Organometallics* **2012**, *31*, 7332–7335.
- [8] K. Zhang, J. Prabhavathy, J. H. K. Yip, L. L. Koh, G. K. Tan, J. J. Vittal, *J. Am. Chem. Soc.* **2003**, *125*, 8452–8453.
- [9] R. Uson, A. Laguna, M. V. Castrillo, *Synth. React. Inorg. Met.-Org. Chem.* **1979**, *9*, 317–324.
- [10] a) H. Schmidbaur, A. Hamel, N. W. Mitzel, A. Schier, S. Nogai, *Proc. Natl. Acad. Sci. USA* **2002**, *99*, 4916–4921; b) A. Hamel, N. W. Mitzel, H. Schmidbaur, *J. Am. Chem. Soc.* **2001**, *123*, 5106–5107; c) A. Bayler, A. Bauer, H. Schmidbaur, *Chem. Ber.* **1997**, *130*, 115–118.
- [11] S. G. Weber, F. Rominger, B. F. Straub, *Eur. J. Inorg. Chem.* **2012**, 2863–2867.
- [12] A. Slade, H. Schmidbaur, *Z. Naturforsch. B* **1997**, *52b*, 301–303.
- [13] X. Shi, D. J. Gorin, F. D. Toste, *J. Am. Chem. Soc.* **2005**, *127*, 5802–5803.
- [14] a) N. Mézailles, L. Ricard, F. Gagosz, *Org. Lett.* **2005**, *7*, 4133–4136; b) M. Preisenberger, A. Schier, H. Schmidbaur, *J. Chem. Soc. Dalton Trans.* **1999**, 1645–1650; c) S. Komiya, J. K. Kochi, *J. Organomet. Chem.* **1977**, *135*, 65–72. In contrast, a gold triflate with a unique di(*c*-hexyl)phosphine ligand with a shielding arene substituent could be isolated: d) S. Doherty, J. G. Knight, A. S. K. Hashmi, C. H. Smyth, N. A. B. Ward, K. J. Robson, S. Tweedley, R. W. Harrington, W. Clegg, *Organometallics* **2010**, *29*, 4139–4147.
- [15] The digold complexes were occasionally isolated accidentally from enol ether π -complex preparation solutions, but could also be prepared efficiently according to Schmidbaur's procedure, ref. [10].
- [16] X-ray crystallographic data for **1-CH₂Cl₂**: C_{20.50}H₂₈Ag_{0.50}Au_{11.50}F₆PSb; *M* = 845.23; orthorhombic; *Pnma*; *T* = 193(2) K; *a* = 26.955(3), *b* = 18.011(2), *c* = 10.5823(13) Å; β = 90°; *V* = 5137.6(11) Å³; *Z* = 8; *R*₁ [*I* > 2 σ (*I*)] = 0.0368; *wR*₂(*F*²) = 0.0998;

- GOF=1.035. For $2 \cdot \frac{1}{2} \text{H}_2\text{O}$: $\text{C}_{40}\text{H}_{55}\text{Au}_2\text{F}_6\text{O}_{50}\text{P}_2\text{Sb}$; $M=1270.91$; triclinic; $P\bar{1}$; $T=193(2)$ K; $a=11.339(2)$, $b=14.874(3)$, $c=15.208(3)$ Å; $\beta=111.092(2)^\circ$; $V=2207.8(7)$ Å³; $Z=2$; $R1$ [$I > 2\sigma(I)$]=0.0566; $wR2(F^2)=0.1205$; GOF=0.964. For $3 \cdot \text{CH}_2\text{Cl}_2$: $\text{C}_{25}\text{H}_{36}\text{Au}_2\text{Cl}_3\text{F}_6\text{P}_2\text{Sb}$; $M=1154.67$; monoclinic; $P12_1/c1$; $T=193(2)$ K; $a=8.0567(11)$, $b=17.237(2)$, $c=27.728(4)$ Å; $\beta=94.451(2)^\circ$; $V=3839.1(9)$ Å³; $Z=4$; $R1$ [$I > 2\sigma(I)$]=0.0492; $wR2(F^2)=0.1058$, GOF=1.009. CCDC-933198 ($1 \cdot \text{CH}_2\text{Cl}_2$), CCDC-933199 ($2 \cdot \frac{1}{2} \text{H}_2\text{O}$), and CCDC-933200 ($3 \cdot \text{CH}_2\text{Cl}_2$) contain the supplementary crystallographic data for this paper. These data can be obtained free of charge from The Cambridge Crystallographic Data Centre via www.ccdc.cam.ac.uk/data_request/cif
- [17] a) H. Schmidbaur, A. Schier, *Chem. Soc. Rev.* **2012**, *41*, 370–412; b) H. Schmidbaur, A. Schier, *Chem. Soc. Rev.* **2008**, *37*, 1931–1951.
- [18] a) E. Herrero-Gómez, C. Nieto-Oberhuber, S. López, J. Benet-Buchholz, A. M. Echavarren, *Angew. Chem.* **2006**, *118*, 5581–5585; *Angew. Chem.* **2006**, *118*, 5581–5585; b) P. Pérez-Galán, N. Delpont, E. Herrero-Gómez, F. Maseras, A. M. Echavarren, *Chem. Eur. J.* **2010**, *16*, 5324–5332.
- [19] A. Bondi, *J. Phys. Chem.* **1964**, *68*, 441–451.
- [20] S. V. Lindeman, R. Rathore, J. K. Kochi, *Inorg. Chem.* **2000**, *39*, 5707–5716.
- [21] N. Savjani, D.-A. Roşca, M. Schormann, M. Bochmann, *Angew. Chem.* **2013**, *125*, 908–911; *Angew. Chem. Int. Ed.* **2013**, *52*, 874–877.
- [22] A. V. Vasilyev, S. V. Lindeman, J. K. Kochi, *Chem. Commun.* **2001**, 909–910.
- [23] K. Matsumoto, R. Hagiwara, Y. Ito, O. Tamada, *J. Fluorine Chem.* **2001**, *110*, 117–122.
- [24] We found inconsistent details on the literature-reported shifts and J_{CP} coupling constants of the parent phosphine gold chloride; our 2D NMR characterization is included in the Supporting Information.
- [25] See Experimental Section and Supporting Information for more details.
- [26] H. G. Raubenheimer, H. Schmidbaur, *Organometallics* **2012**, *31*, 2507–2522.
- [27] T. J. Robilotto, J. Bacsá, T. G. Gray, J. P. Sadighi, *Angew. Chem.* **2012**, *124*, 12243–12246; *Angew. Chem. Int. Ed.* **2012**, *51*, 12077–12080.
- [28] F. Scherbaum, A. Grohmann, B. Huber, C. Krüger, H. Schmidbaur, *Angew. Chem.* **1988**, *100*, 1602–1604; *Angew. Chem. Int. Ed. Engl.* **1988**, *27*, 1544–1546.
- [29] A. N. Nesmeyanov, E. G. Perevalova, Y. T. Struchkov, M. Y. Antipin, K. I. Grandberg, V. P. Dyadhenko, *J. Organomet. Chem.* **1980**, *201*, 343–349.
- [30] a) G. A. Olah, G. Rasul, M. Hachoumy, A. Burrichter, G. K. S. Prakash, *J. Am. Chem. Soc.* **2000**, *122*, 2737–2741; b) G. A. Olah, D. A. Klumpp in *Superelectrophiles and Their Chemistry*, Wiley, Hoboken, **2008**, p. 120.
- [31] a) C. Topf, S. Leitner, U. Monkowius, *Acta Crystallogr. Sect. E* **2012**, *68*, m272; b) X. Wang, S. Liu, L.-H. Weng, G.-X. Jin, *Organometallics* **2006**, *25*, 3565–3569.
- [32] M. C. Blanco, E. J. Fernández, M. E. Olmos, O. Crespo, A. Laguna, P. G. Jones, *Organometallics* **2002**, *21*, 2426–2429.
- [33] J. P. Perdew, K. Burke, M. Ernzerhof, *Phys. Rev. Lett.* **1996**, *77*, 3865–3868.
- [34] In computations on geminally diaurated gold(I) aryls, the PBE0 functional was used and the gold–gold distances were constrained in order to achieve a good fit: E. Heckler, M. Zeller, A. D. Hunter, T. G. Gray, *Angew. Chem.* **2012**, *124*, 6026–6030; *Angew. Chem. Int. Ed.* **2012**, *51*, 5924–5928.
- [35] J.-D. Chai, M. Head-Gordon, *Phys. Chem. Chem. Phys.* **2008**, *10*, 6615–6620.
- [36] For use of the earlier generation ω B97X functional with gold clusters, see: J. V. Koppen, M. Hapka, M. M. Szczęśniak, G. Chałasiński, *J. Chem. Phys.* **2012**, *137*, 114302–114315.
- [37] H. Fang, X.-G. Zhang, S.-G. Wang, *Phys. Chem. Chem. Phys.* **2009**, *11*, 5796–5804.
- [38] a) I. Mayer, *Chem. Phys. Lett.* **1983**, *97*, 270–274; b) I. Mayer, *Int. J. Quantum Chem.* **1984**, *26*, 151–154; c) A. J. Bridgeman, G. Cavigliasso, L. R. Ireland, J. Rothery, *J. Chem. Soc. Dalton Trans.* **2001**, 2095–2108.
- [39] A “non-negligible” MBO of 0.14 was also computed for an NHC dinuclear gold hydroxide and used as evidence of a gold–gold interaction: R. S. Ramón, S. Gaillard, A. Poater, L. Cavallo, A. M. Z. Slawin, S. P. Nolan, *Chem. Eur. J.* **2011**, *17*, 1238–1246.
- [40] The CDA was made using the Multiwfn Program version 2.6.1. For the introduction of Multiwfn 2.1.2 see: T. Lu, F. Chen, *J. Comput. Chem.* **2012**, *33*, 580–592.
- [41] S. Dapprich, G. Frenking, *J. Phys. Chem.* **1995**, *99*, 9352–9362.
- [42] L. Gao, M. A. Peay, D. V. Partyka, J. B. Updegraff III, T. S. Teets, A. J. Esswein, M. Zeller, A. D. Hunter, T. G. Gray, *Organometallics* **2009**, *28*, 5669–5681.
- [43] a) A. E. Reed, L. A. Curtiss, F. Weinhold, *Chem. Rev.* **1988**, *88*, 899–926; b) A. E. Reed, R. B. Weinstock, F. Weinhold, *J. Chem. Phys.* **1985**, *83*, 735–746.
- [44] K. B. Wiberg, *Tetrahedron* **1968**, *24*, 1083–1096.
- [45] A. S. K. Hashmi, M. C. Blanco, E. Kurpejović, W. Frey, J. W. Bats, *Adv. Synth. Catal.* **2006**, *348*, 709–713.
- [46] a) A. D. Becke, *J. Chem. Phys.* **1993**, *98*, 5648–5653; b) A. D. Becke, *Phys. Rev. A* **1988**, *38*, 3098–3100; c) C. Lee, W. Yang, R. G. Parr, *Phys. Rev. B* **1988**, *37*, 785–789.
- [47] M. Dolg, U. Wedig, H. Stoll, H. Preuss, *J. Chem. Phys.* **1987**, *86*, 866–872.

Received: June 5, 2013

Published online: August 9, 2013